THE JOURNAL OF PHYSICAL CHEMISTRY B

Article

pubs.acs.org/JPCB

Spontaneous Formation of Vesicles by Self-Assembly of Cationic Block Copolymer in the Presence of Anionic Surfactants and Their Application in Formation of Polymer Embedded Gold Nanoparticles

Rakesh Banerjee, Sujan Dutta, Souvik Pal, and Dibakar Dhara*

Department of Chemistry, Indian Institute of Technology Kharagpur, West Bengal 721302, India

ABSTRACT: Block copolymers (BCPs), synthesized from cationic monomer (3-(methacryloylamino)propyl)-trimethylammonium chloride (MAPTAC) and PEG-based monomer poly(ethylene glycol) methyl ether acrylate (PEGMEA), were found to spontaneously form water-soluble vesicles when mixed with a stoichiometric quantity of negatively charged double-tail surfactant, AOT, at room temperature. However, with single-tail anionic surfactant, i.e., SDS, these block copolymers were seen to form water-soluble micelle-like aggregates. Also, cationic random copolymers (RCPs) of similar composition synthesized from the same monomers showed formation of water-soluble micelle-like aggregates when complexed with SDS or AOT. Such self-assembled vesicle formation observed specifically for the BCP/AOT systems was attributed to a sequential arrangement of monomers in the BCP and the higher hydrophobic volume of AOT, that made the packing factor "*p*" assume a value that favors the formation of vesicles. TEM analysis showed that average diameters of the vesicles were in the range of ∼100 nm. Pyrene fluorescence experiments indicated a high degree of hydrophobicity of vesicle membrane made from BCP/AOT complexes which were even higher than that of the cores of the water-soluble micelle-like aggregates made from BCP/SDS, RCP/AOT, and RCP/SDS systems. Importantly, the vesicles made from these BCP/AOT stoichiometric complexes were successfully utilized to reduce $HAuCl_4$ to gold nanoparticles. TEM analysis revealed that the gold nanoparticles so formed were successively embedded within the hydrophobic bilayer shell of the vesicles.

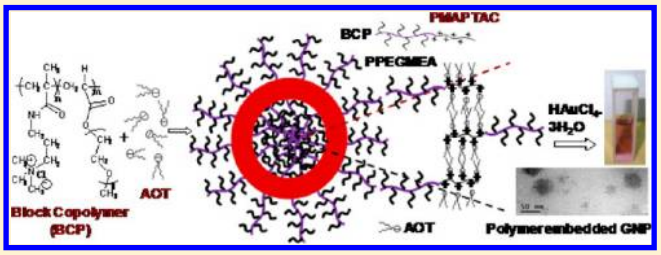

INTRODUCTION

Polymer vesicles or polymersomes, made of amphiphilic copolymers, usually possess an aqueous interior separated from the outside by a hydrophobic membrane with both external and internal surfaces formed by hydrophilic shells.[1−4] Compared to lipid-based vesicles,[5] these polymersomes are more soluble and robust and hence have the potential for more advanced physiological applications.[6] Therefore, there has been a significant research interest around the designing, synthesis, and modification of polymer vesicles for a wide range of applications, ranging from materials science to biomedical science.[7] Applications of polymersomes as carriers for drugs and other therapeutic agents are perhaps the most promising of all biomedical applications. Polymersomes have attracted considerable attention as vehicles for drug and gene delivery, especially in cancer therapy, mainly due to their dual advantage offered by their hydrophilic core as well as hydrophobic shell.[8−11] The hydrophobic bilayer membrane that forms the vesicle wall helps in sequestering and trapping hydrophobic moieties, e.g., dye molecules, that in turn aids in the tracking and imaging of these nanocarriers when used as drug-delivery vehicles.[6,12,13] In addition, unlike normal polymeric micelles, these vesicles can also encapsulate hydrophilic molecules into their aqueous interior. Besides, it is equally important for the drug encapsulated polymersomes to release the therapeutic agents at the specific pathological site. In this regard, a hydrophilic shell containing poly(ethylene glycol) (PEG) has attracted significant attention due to its excellent biocompatibility that imparts a prolonged lifetime to the polymersomes in the bloodstream, and also helps them to attain an enhanced permeability and retention (EPR) effect at the site of a solid tumor.[14−16] Hence, design and preparation of robust polymersomes containing a PEG shell as vehicles for controlled drug-delivery is an extremely important topic in today's perspective.

Among the numerous polymers that have been used for the preparation of polymer vesicles, amphiphilic block copolymers are the most promising materials that are capable of forming vesicles by the self-assembly process. In general, there are two methods for the preparation of polymer vesicles via self-assembly of block copolymers. One of them is the "solvent-switch" method, where the copolymer is dissolved in an organic solvent prior to self-assembly.[17] In the second method, only water is required for the dissolution of the block copolymers, leading to self-assembly.[18] However, both methods are very tedious and time-consuming. Kataoka and co-workers have reported that the mixing of two oppositely charged block copolymers in aqueous solution afforded the formation of polymer vesicles with a semipermeable polyion complex

Received: October 4, 2012
Revised: March 4, 2013
Published: March 7, 2013

   dx.doi.org/10.1021/jp309808q | *J. Phys. Chem. B* 2013, 117, 3624−3633

membrane.[19,20] Block ionomer complexes (BICs), synthesized by reacting double hydrophilic block copolymers containing a polyion chain and a water-soluble nonionic chain with surfactants of opposite charge, were found to be forming polymersomes spontaneously in aqueous medium.[21,22] These approaches provide a simplified procedure for the preparation of well-defined polymer vesicles. In the present work, we report spontaneous formation of polymer vesicles by complexation of cationic block copolymers (BCPs) with PEG brush synthesized using different mole ratios of poly(ethylene glycol)methyl ether acrylate (PEGMEA) and (3-(methacryloylamino)propyl)-trimethylammonium chloride (MAPTAC) (Scheme 1), with oppositely charged double tail surfactant, AOT.

Scheme 1. (a) Cationic Random Copolymers from MAPTAC and PEGMEA (RCPs) and (b) Cationic Block Copolymers (BCPs) of MAPTAC and PEGMEA Using MAPTAC Macro-CTA Agent

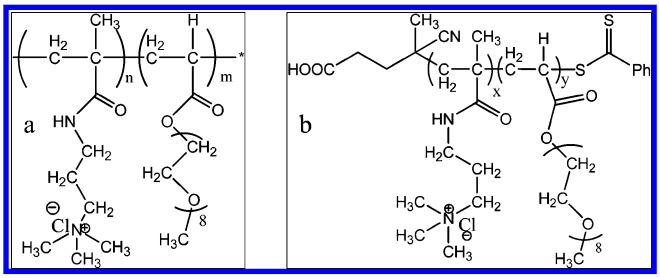

Besides, we have also explored the possibility of formation of stable polymer embedded gold nanoparticles by the BCP/AOT polymer vesicles. A specific advantage of polymer embedded gold nanoparticles compared to self-assembled polymer vesicles is their ease of detection. Freese et al. by using gold nanoparticles as the core for the particles showed that it is possible to visualize directly intracellular distribution and also quantify cellular uptake, without the need for additional biomarkers or fluorescent labels.[23] They also clearly demonstrated that, by changing the nanoparticle size and the type of polymer coating, uptake behavior in endothelial cells can be modulated without causing cytotoxicity. Hence, polymer vesicles or polymersomes embedded with gold nanoparticles are quite significant with respect to their biological usefulness. In the present work, we show that the BCP/AOT polymer vesicles were able to reduce $HAuCl_4$ and stabilize the resulting gold nanoparticles. In this study, we have also investigated the complexation behavior of the BCPs with single-tail anionic surfactant, SDS, as well as the complexation of random cationic copolymers (RCPs) of similar compositions as the BCPs, with both AOT and SDS. A thorough characterization of the resulting complexes has been done in order to understand the fundamentals of the complexation behavior. The selective formation of vesicular structures by specific polymer−surfactant systems has also been logically addressed.

EXPERIMENTAL SECTION

Materials. Poly(ethylene glycol) monomethyl ether acrylate (PEGMEA, MW 480), (3-(methacryloylamino)propyl)-trimethyl ammonium chloride (MAPTAC; 50 wt % solution in water), 2,2′-azo-bis(2-amidinopropane)dihydrochloride (V-501), sodium bis(2-ethylhexyl)sulfosuccinate (AOT), pyrene, and gold(III) chloride trihydrate ($HAuCl_4 \cdot 3H_2O$) were purchased from Aldrich Chemicals and used as received. Benzyl chloride, potassium hexacyano ferrate, HPLC grade water, and all other solvents used were purchased from SRL and Spectrochem (India). 4-Cyanopentanoic acid dithiobenzoate (CPABD) was synthesized according to the literature procedure.[24] All aqueous solutions were prepared using Milli-Q water.

Synthesis of Cationic Block Copolymers Using MAPTAC and PEGMEA (BCPs). Details of the block copolymer synthesis by the aqueous RAFT polymerization technique has been reported by us elsewhere.[25] Briefly, in the first step, controlled synthesis of poly(MAPTAC) was done at 70 °C using V-501 as the primary radical source and CPABD as the chain-transfer agent. The polymerization was performed in an aqueous acetic buffer (pH 5.2; 0.27 mol L^{-1} acetic acid and 0.73 mol L^{-1} sodium acetate) with a monomer to CTA ratio ($[M]_0/[CTA]_0$) of 200:1 and a CTA to initiator ratio ($[CTA]_0/[I]_0$) of 4:1. The molecular weight of the resulting poly(MAPTAC) was determined by integration of the five protons of the phenyl ring of the terminal RAFT agent with respect to trimethyl protons of MAPTAC repeat units. In the next step, controlled polymerization of PEGMEA was done using the first block, i.e., poly(MAPTAC), as macro-CTA in an aqueous acetic buffer (pH 5.2, 0.27 mol L^{-1} acetic acid and 0.73 mol L^{-1} sodium acetate) using three different ratios of the monomer PEGMEA and poly(MAPTAC) macro-CTA. The ratio of macro-CTA to initiator ratio was fixed at 3:1 in all three cases. We could not synthesize a block copolymer of target composition of 5:95 (in mol %) [MAPTAC: PEGMEA], possibly due to the very low required concentration of poly(MAPTAC) macro-CTA with respect to PEGMEA monomer (1:1200) that results in a homopolymerization of PEGMEA with a loss of control over molecular weight as well as PDI. The compositions of the block copolymers were determined by integration of the relative intensities of methylene-protons adjacent to ester oxygen of the PPEGMA block with chemical shift value at 4.2 ppm and intensities of the protons adjacent to the quaternary nitrogen in

Table 1. Composition and Molecular Weight Data of the Polymers in This Study

	polymer composition[a] (mol %)						
polymer	MAPTAC	PEGMEA	Mn[a] (g/mol)	Mn[c]	PDI[c]	no. of MAPTAC structural units in the block[a]	no. of PEGMEA structural units in the block[a]
BCP-31[b]	31.0	69.0	104 000	112 000	1.37	80	178
BCP-16[b]	16.0	84.0	220 000	194 000	1.46	80	420
RCP-36	36.0	64.0		103 000	2.93		
RCP-14	14.0	86.0		142 000	2.84		
RCP-5	5.0	95.0		174 000	3.16		

[a]From ^{1}H NMR. [b]From ref 25. [c]From GPC.

dx.doi.org/10.1021/jp309808q | J. Phys. Chem. B 2013, 117, 3624−3633

the PMAPTAC block with chemical shift value at 3.0 ppm. The molecular weight of the second block, PPEGMA, was determined from the copolymer composition determined as above and from the knowledge of the molecular weight of the PMAPTAC block. Gel permeation chromatography was done using HPLC water containing 0.1 wt % NaCl as the mobile phase, and MWs were reported with respect to PEG/PEO standards. The composition and molecular weights of the BCPs are provided in Table 1.

Synthesis of Cationic Random Copolymers Using MAPTAC and PEGMEA (RCPs). A series of RCPs were synthesized by free radical polymerization of PEGMEA and MAPTAC in water (total monomer concentration ∼4 wt %) at 60 °C using V-501 as the primary radical source. Sodium chloride was added to the monomer solution to make a salt concentration of 1×10^{-3} M. Compositions of the RCPs were chosen to match the compositions of similar PEG containing random copolymers reported in the literature so that the present data can be compared with literature data.[26−29] Polymerization was carried out in a septum sealed round bottomed flask that was purged with nitrogen for 30 min prior to polymerization. Polymerization was carried out for 20 h at 60 °C followed by termination by immersing the reaction flask in liquid nitrogen. The resulting polymers were dialyzed against Milli-Q water using cellulose membrane (cut off 12 400 D) for 7 days. The purified copolymer was freeze-dried and characterized by ^{1}H NMR spectroscopy and GPC. The molecular weights were determined by GPC, and the copolymer compositions of the copolymers were calculated by integration of relative normalized resonances of the methylene-proton peaks at 4.2 ppm (PPEGMEA) with trimethyl proton (PMAPTAC) at 2.9 ppm. Final compositions of the copolymers were very close to the monomer feed compositions. A similar procedure for synthesis of poly(ethylene glycol) methacrylate based RCPs was reported earlier.[26] Molecular weights and the composition of the RCPs are listed in Table 1.

Preparation and Characterization of Polyelectrolyte−Surfactant Complexes. The polyelectrolyte−surfactant complexes were prepared by mixing the aqueous solutions of the copolymers (BCPs and RCPs) synthesized and the surfactants (AOT and SDS). As AOT has a relatively low solubility in water, AOT stock solutions were prepared in methanol. In all cases, the concentration of methanol in the final solution did not exceed 0.25 vol %. The stability of polymer−surfactant complexes remains unaffected at this level of alcohol concentration.[30] The polymer−surfactant complexes are labeled according to the composition of the mixture; for example, BCP/AOT complexes refer to the complex formed from the mixture of the cationic block copolymers and AOT. Turbidity measurements, reported as $(100 - \%T)/100$, where T is the transmittance, were carried out at 420 nm using UV−vis spectroscopy (Shimadzu UV−vis Spectrophotometer, model no. UV2450) at 25 °C. The measured turbidity values were corrected by subtracting the turbidity of the polymer-free blank. The turbidity values were recorded after the values became stable. For fluorescence measurements, the concentration of pyrene was held constant at 1.0×10^{-6} M. A 2 mL portion of each solution was placed in a 10 mm rectangular quartz cell, and the spectra were run in a SPEX-Fluorolog-3 spectrophotometer in right angle geometry using slit openings of 2 mm. Pyrene was excited at 339 nm, and emissions at 376 and 386 nm were taken as the first and third vibronic peaks (known as I_1 and I_3, respectively). It is known that the value of I_1/I_3 correlates well with the polarity of the immediate environment of the pyrene molecule.[31] The emission spectra were accumulated with an integration time of 1.0 s/0.5 nm. A negative staining technique was used for the transmission electron microscopy (TEM) studies of the polymer−surfactant complexes. A drop of the sample solution was allowed to settle on a carbon coated copper grid for 1 min. Excess sample was wiped away with filter paper, and a drop of 1% uranyl acetate solution in methanol was allowed to come in contact with the sample for 1 min. The samples were air-dried and analyzed using a JEOL JEM 100CX microscope operating at 80 kV. The hydrodynamic diameter (R_H) of the polyelectrolyte−surfactant complex was obtained from dynamic light scattering (DLS) at 22 °C using a Malvern Nano ZS instrument employing a 4 mW He−Ne laser operating at a wavelength of 633 nm. Copolymer solutions of 1 g L^{-1} in water were titrated against the appropriate amount of AOT solutions, by stepwise addition of 3 μL aliquots. All samples were filtered through a membrane filter with a pore size of 0.2 μm before DLS measurement. Initial measurements were taken to estimate the working concentration of the polymer and surfactants at which there is no sign of aggregation. ζ-Potential measurements were performed at 22 °C using a Malvern Nano ZS instrument employing a 4 mW He−Ne laser operating at a wavelength of 633 nm. Typically, a solution of 1 g L^{-1} copolymer in water was titrated against the appropriate AOT solutions, by the stepwise addition of 3 μL aliquots.

Preparation and Characterization of Gold Nanoparticles. Gold nanoparticles were prepared by mixing an aqueous 0.01 mol L^{-1} hydrogen tetrachloroaurate (III) hydrate ($HAuCl_4 \cdot 3H_2O$) solution with aqueous solutions containing copolymer−surfactant complexes so that the final concentration of $AuCl_4^-$ was 1.0×10^{-4} mol L^{-1}. The concentration of polymers in the final solution was 1.0 g L^{-1}, and the appropriate amount of surfactant solution was added to make the charge ratio, Z_-/Z_+, 1.0. The solutions were left standing at 35 °C under magnetic stirring, and absorbance was noted at different time intervals. The size of the synthesized gold nanoparticles was obtained from TEM measurement operating at 200 kV.

RESULTS AND DISCUSSION

Well-defined block copolymers were synthesized from cationic monomer (3-(methacryloylamino)propyl)trimethylammonium chloride (MAPTAC) and PEG-based monomer poly(ethylene glycol) methyl ether acrylate (PEGMEA) using controlled radical polymerization. The details of the polymerization have been reported earlier.[25] Random copolymers of similar composition were also prepared using the same monomers using conventional radical polymerization. Turbidimetric titration was used to determine the solubility of polymer surfactant complexes at various compositions in aqueous media. As seen from the turbidimetric data plotted against the charge ratio Z_-/Z_+ (Figure 1a and 1b), all the polyelectrolyte−surfactant complexes were practically optically transparent for all values of Z_-/Z_+ examined. There was no macroscopic phase separation observed for either the BCPs or the RCPs when complexed with SDS and AOT even at sufficiently high concentration of the polyelectrolytes. The charge ratio, Z_-/Z_+, is expressed as the ratio of surfactant concentration, C_s, to the concentration of charge groups in the polyelectrolyte (C_p), i.e., $Z_-/Z_+ = C_s/C_p$. Generally speaking, the tendency of these polyelectrolyte-oppositely charged surfactant systems to phase separate from aqueous medium as a result of charge

dx.doi.org/10.1021/jp309808q | J. Phys. Chem. B 2013, 117, 3624−3633

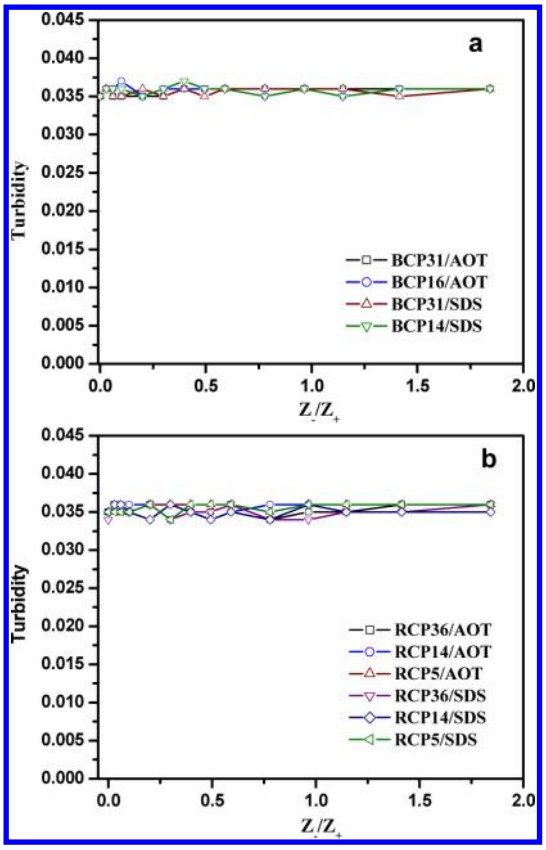

Figure 1. Variation of turbidity as a function of charge ratio, Z_-/Z_+, for (a) BCP/surfactant complexes and (b) RCP/surfactant complexes. The polymer concentration was kept constant at 1.0 g L^{-1}. Turbidity values are reported as $(100 - \%T)/100$, where T is the transmittance.

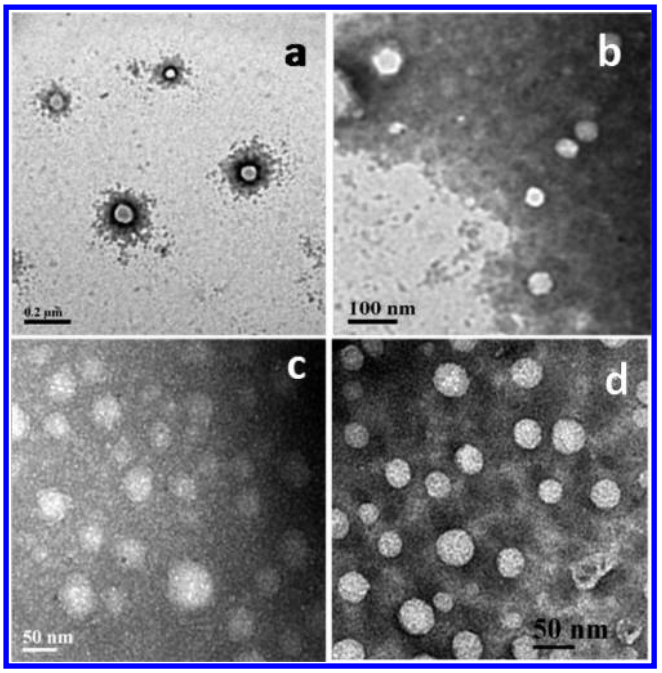

Figure 2. Transmission electron micrograph of (a) BCP-31/AOT, (b) BCP-16/AOT, (c) BCP-31/SDS, and (d) RCP-36/AOT complexes at a charge ratio of $Z_-/Z_+ = 1$. The length of the bar shown in the figure is as follows: (a) 200 nm, (b) 100 nm, (c) 50 nm, and (d) 50 nm.

neutralization has hindered the use of these complexes in nanomedicines.[32] The solubility of the presently studied polyelectrolyte−surfactant complexes even at the electroneutrality point must have resulted from the lyophilizing effect of the pendant PEG segments of the copolymers. Random copolymers synthesized from poly(ethylene glycol) mono methyl ether methacrylate and MAPTAC have been reported to form water-insoluble complexes with SDS and AOT when the content of MAPTAC was relatively high (32−34 mol %).[26,29] A similar behavior was also observed for poly(ethylene oxide)-*block*-poly(sodium methacrylate) with cetylpyridinium bromide (CPB) complex [CPB/PEO(30)-*b*-PMA(147)].[33] Thus, the fact that we could achieve complete solubility for all systems we studied indicated that PEGMEA has a relatively higher lyophilizing effect than the corresponding methacrylate macro-monomer possibly due to absence of the additional methyl group that is present in the latter.

Complexation of BCPs with Surfactants. Electron microscopy was used to determine the size and shape of the polyelectrolyte−surfactant complexes formed by stoichiometric quantities of polyelectrolyte and surfactants, i.e., $Z_-/Z_+ \sim 1$. The TEM analysis of the BCPs with AOT produced interesting results, as evident from Figure 2a. BCP-31 formed vesicular structures on complexation with AOT. In the case of the BCP-16/AOT system, the TEM micrographs (Figure 2b) revealed coexistence of both vesicles and micelle-like aggregates. Thus, BCP effectively interacted with AOT, resulting in spontaneous formation of vesicles with a corona consisting of segregated chains of the block copolymer and the oppositely charged AOT molecules. The average diameter of the spherical vesicles was ∼100 nm. TEM analysis revealed that complexation of the BCPs with SDS resulted in the formation of simple micelle-like aggregates, as shown in Figure 2c.

Complexation of RCP with Surfactants. Besides studying the complexation leading to nanostructure formation resulting from interaction of cationic block-copolymer with single- and double-chain anionic surfactant, we also tried to investigate the effect of randomness of the copolymer structure on such nanostructure formation. Comparison of the interaction behavior of block and random copolymers having similar compositions with surfactants are scarce in the literature. The random copolymers synthesized in the present work, RCP-14 and RCP-36, were mixed with AOT as well as with SDS, and the resulting complexes were characterized using TEM analysis. Both of the RCPs were seen to form nanosized spherical aggregates with an average diameter in the range 30−40 nm. Figure 2d shows the representative electron micrograph of the RCP-36/AOT complex at a charge ratio of $Z_-/Z_+ \sim 1$. Our result is in agreement with the formation of similar water-soluble micelle-like aggregates using similar types of cationic random copolymers and oppositely charged surfactants reported earlier.[26−29]

It is interesting to note from the above results that the feasibility of formation of vesicles by the spontaneous self-assembly process was specific to the block copolymer architecture of a polyelectrolyte and also the presence of a double hydrophobic tail in the surfactant, as in the case of the BCP/AOT system. Any variation from this renders the complex incapable of forming a vesicular structure, although core−shell type micelle-like aggregates which are soluble in water are formed in those systems. Such special behavior by BCP/AOT systems may be explained on the basis of the packing parameter "p" value. Classically, a dimensionless packing parameter "p" is defined as[34] $p = \nu/a_0 l_c$, where ν is

dx.doi.org/10.1021/jp309808q | J. Phys. Chem. B 2013, 117, 3624−3633

the volume of the hydrophobic segment, a_0 is the contact area of the headgroup with solvent, and l_c is the length of the hydrophobic segment. It is primarily the "p" value that determines the morphology of the self-assembled nanostructure. It is obvious that a given molecule does not have a fixed packing parameter value, as all three factors, ν, a_0, and l_c, depend on the conditions under which self-assembly takes place. Factors which control the nanostructure morphology include the chemical structure of the copolymer, the hydrophilic volume to hydrophobic volume ratio, the concentration of copolymer in solution, and the solvent properties such as the type of organic solvent and the ratio of organic solvent to water, salt concentration, solution pH, and temperature.[17] Among these factors, the volume ratio of the hydrophilic to hydrophobic block is proposed to be an extremely important parameter in determining the self-assembled structures. As a general rule, when $p < 1/3$, spheres are formed; when $1/3 < p < 1/2$, cylinders; when $1/2 < p < 1$, flexible lamellae or vesicles; finally, when $p = 1$, planar lamellae. From the knowledge of the aggregation properties of amphiphilic copolymers,[26,35,36] it can be stated here that the polyelectrolyte−surfactant systems studied by us form micelle-like aggregates in water with a core made of surfactant-neutralized PMAPTAC blocks and a shell composed of the PEG blocks. The BCPs studied here consist of two hydrophilic blocks—poly(PEGMEA) containing PEG grafts and poly(MAPTAC) bearing all the cationic charges. On complexation with anionic surfactants, the positive charges of the poly(MAPTAC) block get neutralized, making the particular block hydrophobic. As a result, the block copolymer−surfactant complex spontaneously self-assembles in order to hide the hydrophobic block from the aqueous medium. SDS with its linear C_{12} tail has a relatively lower volume of the hydrophobic portion as compared to AOT with two branched hydrophobic tails.

Hence, complexation of the poly(MAPTAC) block with SDS results in a hydrophobic segment having comparatively low volume (ν), yielding a "p" value that supported micellar structure, whereas AOT, owing to its double and branched hydrophobic tails, complexes with poly(MAPTAC) to yield a comparatively larger volume of the hydrophobic portion. This led to an increased "p" value that supported formation of nanostructured vesicles. Again, the block length of the poly(PEGMEA) block is higher in BCP-16 than in BCP-31, whereas the length of the poly(MAPTAC) blocks in two BCPs is the same (Table 1). Hence, the hydrophilic to hydrophobic volume ratio of the AOT-neutralized complex is higher in the case of BCP-16 than in teh case of BCP-31. As a result, the value of "p" is expectedly lower for the BCP-16 system, which is reflected in the formation of a mixture of vesicles and micelles. A schematic presentation of the vesicle formation for the BCP/AOT system is provided in Scheme 2.

Additional information regarding the size (R_H) and polydispersity of the BCP/AOT complexes was determined by dynamic light scattering (DLS) measurements. Figure 3 shows the hydrodynamic radius as a function of charge ratio (Z_-/Z_+) for the BCP/AOT complexes. The size of the micelle-like aggregates increased with an increase in charge ratio (Z_-/Z_+) until the value of $Z_-/Z_+ \sim 0.8$ was reached beyond which the size did not show any further change. This indicates that, around $Z_-/Z_+ \sim 0.8$, the formation of vesicles took place. The size of the BCP-31/AOT vesicles, as observed from TEM, was slightly lower (~60 nm) than that of the BCP-16/AOT system probably due to the higher molecular weight of the PEG-containing block in BCP-16 than in BCP-31. As the lengths of the cationic block in the two block copolymers are the same, any variation in size of the BCP/AOT complexes may be attributed to the difference in the length of the poly(PEGMEA) block.

Scheme 2. Schematic Representation of Vesicle Formation from BCP/AOT Systems

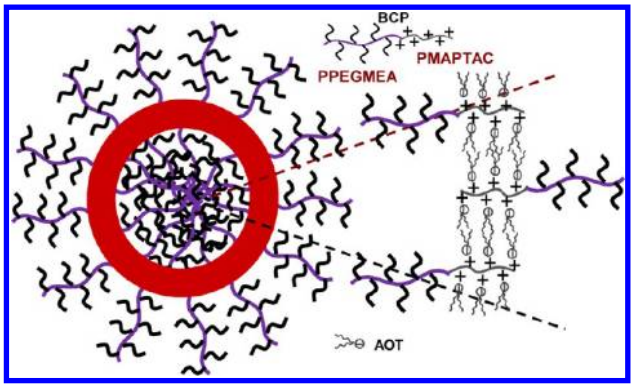

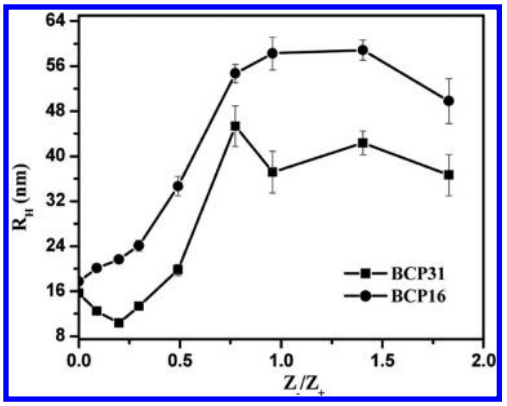

Figure 3. Variation of average diameter as a function of the charge ratio for BCP/AOT complexes. The polymer concentration was kept constant at 1.0 g L^{-1}, and the surfactant concentration was varied to obtain the required charge ratio (Z_-/Z_+). Data reported here are averages of the two repeats.

Fluorescence Study of Polyelectrolyte−Surfactant Binding Equilibrium. The complexation between polyelectrolytes and oppositely charged surfactants is an entropy-driven cooperative process in which the anionic headgroup of surfactant binds with the cationic centers of the polymer, while the alkyl chains of the surfactants segregate to form the hydrophobic domains that may include a hydrophobic polymeric backbone occasionally. The binding of surfactant with polyelectrolytes occurs once the concentration of the surfactant exceeds some critical value termed as the "critical association concentration".[37] As hydrophobic domains are created during the complexation process, fluorescence spectroscopy is successfully employed to track the resulting polarity changes by using pyrene, a fluorescent polycyclic aromatic hydrocarbon, as the hydrophobic probe.[38] The intensity ratio of the first and third vibrational peaks (I_1/I_3 ratio) in pyrene fluorescence spectra is known to be sensitive to the polarity of the medium in which pyrene exists.[31] It is known that pyrene gets partitioned in the hydrophobic domains of an aggregate, and hence monitoring of the I_1/I_3 ratio serves as a measure of the polarity of the microenvironment. In aqueous solution, the I_1/I_3 values lie in the range between 1.7 and 1.9, while, in a non-

dx.doi.org/10.1021/jp309808q | J. Phys. Chem. B 2013, 117, 3624−3633

polar solvent such as hexane, it is about 0.6. The plots of I_1/I_3 values for the BCP−surfactant complexes and the RCP−surfactant systems against charge ratio have been depicted in Figure 4a and b. The I_1/I_3 values for the aqueous solutions of

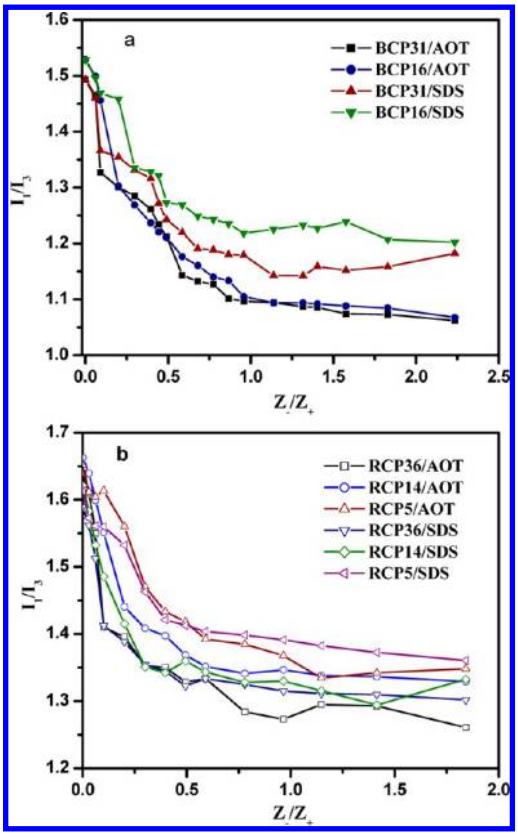

Figure 4. Variation of I_1/I_3 as a function of charge ratio (Z_-/Z_+) for (a) BCP-16 and BCP-31 and (b) RCP-6, RCP-14, and RCP-36. The polymer concentration was kept constant at 1.0 g L^{-1}, and the surfactant concentration was varied.

only BCPs were found to be ∼1.52, while those for the RCPs were ∼1.6, both of which were slightly lower in comparison to the value of 1.72 corresponding to pure water. This indicates that pyrene was experiencing a slightly more hydrophobic environment in the solutions of BCPs and RCP than in pure water. The presence of hydrophobic backbones in the copolymers may have caused a slight decrease in the polarity of the medium. Decrease in the I_1/I_3 values with increase in Z_-/Z_+ for all the polyelectrolyte−surfactant systems indicates the formation of hydrophobic domains as a result of nanoparticle formation through electrostatic interaction.

A significant drop of I_1/I_3 values with a gradual increase in Z_-/Z_+ indicates the formation of hydrophobic domains or micelle-like aggregates due to charge neutralization, in order to minimize their contact with water. Of the two surfactants, the hydrophobic regions formed by complexation of AOT with the polyelectrolytes have lower micropolarity which is in agreement with previously reported results.[29] The results also showed that the BCPs formed more hydrophobic complexes than the RCPs for the same surfactant system. It is also evident that the walls of the vesicles formed by BCP/AOT systems have more hydrophobicity than the cores of the nanostructured micelle-like aggregates formed by BCP/SDS and the RCP/surfactant systems. Hence, the vesicles can be potentially more effective in solubilization and delivery of hydrophobic agents like drugs.

ζ-Potential Measurement of Polyelectrolyte−Surfactant Systems. The effective charge of both the BCP/AOT and RCP/AOT systems was measured using the laser micro-electrophoresis technique. Figure 5a and b represents the

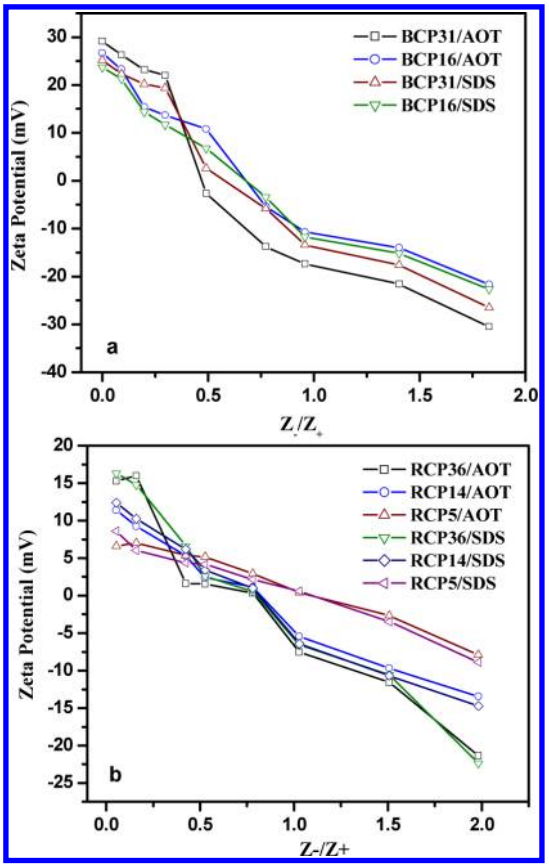

Figure 5. Variation of ζ-potential as a function of the charge ratio in the mixture, Z_-/Z_+, for (a) BCP/AOT and (b) RCP/AOT complexes. The polymer concentration was kept constant at 1.0 g L^{-1}.

variation of ζ-potential as a function of charge ratio (Z_-/Z_+). Initially, for the polyelectrolytes in solution, the ζ-potential shows a positive value and it decreased as the extent of surfactant binding increased. Figure 5a shows that the ζ-potential of BCPs in solution also decreased with increasing AOT concentration. The ζ-potential value of the BCP/AOT complexes showed a more negative value compared to the corresponding RCPs/AOT complexes, and the ζ-potential became zero for Z_-/Z_+ values much lower than 1. This may due to the fact that the positive charges are more closely packed due to their blocky nature and the complexed AOT molecules are closer to each other, thus enabling further association of free AOT molecules through hydrophobic interactions at a lower surfactant AOT concentration. Figure 5b showed that, for the RCP-5/AOT system, the ζ-potential became zero for a Z_-/Z_+ value of 1, whereas, for both RCP-14 and RCP-36 complexes, the ζ-potential became zero for a Z_-/Z_+ value slightly less than 1. This points to the fact that, in the case of RCP-14 and RCP-36, association between the bound and the free AOT molecules through hydrophobic interaction took place before all the cationic charges in the RCPs have electrostatically complexed with AOT. In RCP-5, the cationic

dx.doi.org/10.1021/jp309808q | J. Phys. Chem. B 2013, 117, 3624−3633

charges are well separated and hence the hydrophobic interaction between the bound and the free AOT molecules took place after all the cationic charges were neutralized by AOT. After the stoichiometric ratio, the ζ-potentials of all the BCP/AOT and RCP/AOT systems show a steady negative value due to incorporation of uncomplexed surfactant that was bound to the complex through hydrophobic interaction. Similar behavior was also observed for polyelectrolyte/SDS systems.

Formation and Stabilization of Gold Nanoparticles by BCP/AOT Vesicles. Poly(ethylene glycol) based block copolymers are known to form and stabilize gold nanoparticles.[39−50] Alexandridis et al. demonstrated that poly(ethylene oxide)−poly(propylene oxide)−poly(ethylene oxide) (PEO−PPO−PEO) block copolymers can be used to reduce hydrogen tetrachloroaureate(III) to form gold nanoparticles and stabilize them in aqueous medium.[39−41] Chen et al. proved that the micellization of these block copolymers and hydrophobicity of the micelles were very important for the stabilization of the gold particles.[43] In this piece of work, we explored the possibility of formation of stable gold nanoparticles by utilizing the nanostructured vesicles formed by surfactant-complexed PEG-based random and block copolymers.

Gold nanoparticles were prepared by adding an aqueous solution of 10^{-2} mol L^{-1} $HAuCl_4 \cdot 3H_2O$ at 35 °C to a solution containing stoichiometric quantities of block or random copolymers and AOT or SDS. Final concentrations of polymer and $HAuCl_4 \cdot 3H_2O$ were 1 g L^{-1} and 1.0×10^{-4} mol L^{-1}, respectively. The amount of surfactant solution was added to make the charge ratio $Z_-/Z_+ \sim 1.0$. The solutions were stirred vigorously at the beginning and left standing at 35 °C under gentle magnetic stirring, and absorbance was measured at different time intervals. After mixing $HAuCl_4 \cdot 3H_2O$ solution and BCP-31/AOT stoichiometric complex, the solution turned pink after 2 h, indicating formation of gold nanoparticles in solution. The color of the solution did not change with time; precipitation of particles was not observed even after 15 days, indicating stabilization of gold nanoparticles (Figure 6). Figure 7 shows the representative TEM images of gold nanoparticles formed by the BCP-31/AOT system. The formation of stable polymer-supported gold nanoparticles was confirmed from the TEM pictures and from EDAX analysis. Almost spherical particles of average diameter 10−14 nm were observed.

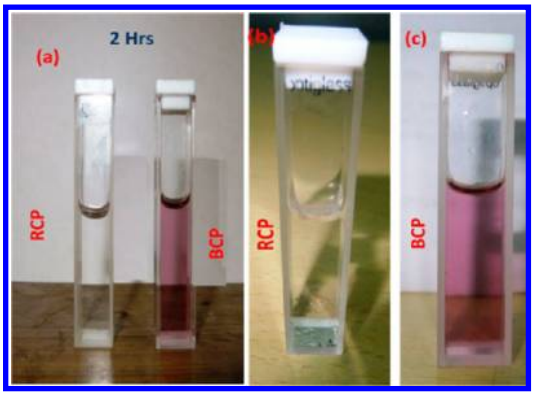

Figure 6. Photographs of (a) formation and stabilization of GNPs for block copolymer by the BCP/AOT complex (BCP) while no formation of GNPs by the RCP/AOT complex (RCP), (b) precipitation of GNPs for RCP/AOT after 7 days, and (c) GNPs for BCP/AOT after 7 days.

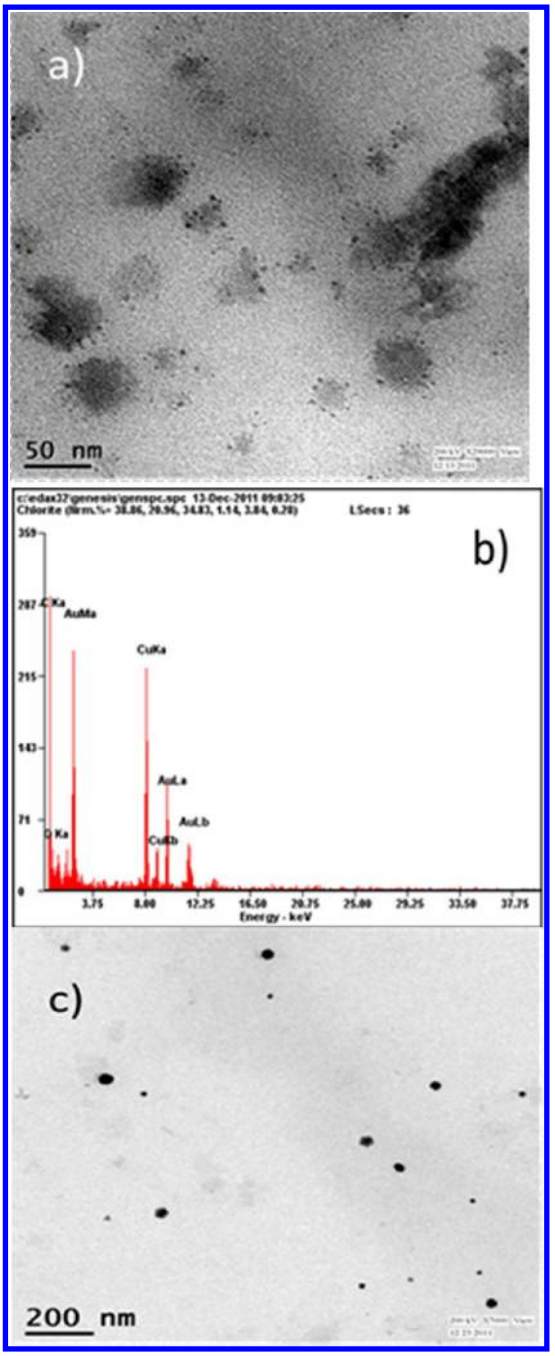

Figure 7. Electron micrographs of gold nanoparticles produced by BCP-31/AOT: (a) polymer supported gold nanoparticles, (b) EDAX analysis for confirmation of gold nanoparticles, and (c) bare gold nanoparticles produced (in very low quantity) in the BCP-31/AOT system.

However, it should be mentioned here that we also found nonencapsulated gold nanoparticles, although in very low quantity, along with polymer supported gold nanoparticles. No particles with a diameter more than 20 nm were observed in both BCP/AOT systems. In the case of the BCP-16/AOT complex, similar color change due to the formation of stabilized gold nanoparticles was also observed after 12 h. However, there was no visual change of color for BCP/SDS complexes and also no precipitation of gold nanoparticles was observed. For the RCP/AOT stoichiometric complexes, there was no visual color change even after 24 h and particulate precipitation occurred

dx.doi.org/10.1021/jp309808q | J. Phys. Chem. B 2013, 117, 3624−3633

after 7 days of being left undisturbed at room temperature (Figure 6). Figure 8 shows the absorbance spectra obtained after 2 h of mixing of an aqueous $AuCl_4^-$ solution and stoichiometric complexes of RCP-36 and BCP-31 with AOT. The absorbance bands centered ~320 and ~535 nm originate from initial gold clusters and surface plasmon of gold nanoparticles, respectively.[42] The prominent absorption band around ~535 nm for the BCP-31/AOT stoichiometric complex after 2 h indicates the formation of stable gold nanoparticles. A similar observation was observed for the BCP-16/AOT system, though the time taken for appearance of a peak for gold nanoparticles was higher (~6 h) than the BCP-31/AOT system. The colloidal stabilization of gold nanoparticles by block copolymer–AOT complexes is most probably due to their amphiphilic character upon complexation and subsequent formation of vesicles in solution. As suggested by Chen et al.,[42] stronger hydrophobic characters of BCP/AOT complexes, as indicated by a lower I_1/I_3 value in pyrene fluorescence, may help in stabilizing the gold nanoparticles. It also explains why BCP-31/AOT complexes were better in stabilizing gold nanoparticles than the BCP-16/AOT system. In th case of BCP/SDS systems, the time taken for appearance of the peak for gold nanoparticles was much higher (more than 12 h) than the BCP/AOT system. A relatively lower hydrophobicity of the BCP/SDS micelle cores compared to BCP/AOT systems is probably the reason for this behavior. Appearance of an absorption band around ~320 nm and absence of any peak around 540 nm for the RCP/AOT complexes indicate initial formation of gold clusters which could not get stabilized by the RCP/AOT system. It was also observed from the absorption spectra that solutions of only the block or the random copolymers in the absence of any surfactant were unable to produce any gold nanoparticles when mixed with an aqueous $AuCl_4^-$ solution. This ruled out the possibility of stabilization of the gold nanoparticles by the terminal thiocarbonyl groups of the block copolymers. Hence, the block copolymer–AOT complexes offer a dual advantage by functioning both as reaction media as well as stabilizer in the process of the formation of stable gold nanoparticles.

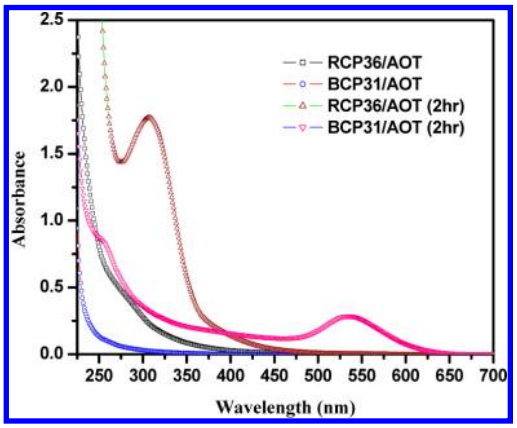

Figure 8. UV–vis absorption spectra of the block and random copolymer solutions, and after 2 h of addition of $HClO_4 \cdot 3H_2O$ in the polymer solutions.

CONCLUSION

Polymersomes or polymer vesicles were produced in water as a result of self-assembly of cationic block copolymers and double-tail anionic surfactant, AOT. These vesicles have highly hydrophobic walls and hydrophilic cores, making them potential candidates as drug-delivery systems. Interaction of block copolymer with single-tailed anionic surfactant, SDS, as well as random copolymer with either AOT or SDS resulted in the formation of micelle-like aggregates. Such variation in nanostructures observed by varying the architecture of a copolymer or the structure of the surfactant could be logically addressed on the basis of possible differences in the value of the packing factor, "*p*", of the surfactant-neutralized block copolymers. An interesting aspect of this vesicle formation selectively by the block copolymer–AOT system was that it could be successfully utilized to form stable gold nanoparticles embedded within the vesicle shells under mild conditions without the need of any other external agents. Such polymer-embedded gold nanoparticles may find useful applications in the field of biological labeling and diagnostics.

AUTHOR INFORMATION

Corresponding Author

*E-mail: dibakar@chem.iitkgp.ernet.in. Phone: +91-3222-282326. Fax: +91-3222-282252.

Notes

The authors declare no competing financial interest.

ACKNOWLEDGMENTS

Financial support from the Department of Science and Technology, Government of India, New Delhi, is acknowledged. R.B. and S.D. acknowledge UGC and CSIR, New Delhi, respectively, for a Junior Research Fellowship. We are also thankful to Prof. Nilmoni Sarkar for some useful discussion.

REFERENCES

(1) (a) Discher, D. E.; Eisenberg, A. Polymer Vesicles. *Science* **2002**, *297*, 967–973. (b) Jain, S.; Bates, F. S. On the Origins of Morphological Complexity in Block Copolymer Surfactants. *Science* **2003**, *300*, 460–464.

(2) (a) Du, J.; O'Reilly, R. K. Advances and Challenges in Smart and Functional Polymer Vesicles. *Soft Matter* **2009**, *5*, 3544–3561. (b) Mai, Y.; Eisenberg, A. Self-Assembly of Block Copolymers. *Chem. Soc. Rev.* **2012**, *41*, 5969–5985.

(3) (a) Binder, W. H.; Barragan, V.; Menger, F. M. Domains and Rafts in Lipid Membranes. *Angew. Chem., Int. Ed.* **2003**, *42*, 5802–5827. (b) Thompson, K. L.; Chambon, P.; Verber, R.; Armes, S. P. Can Polymersomes Form Colloidosomes? *J. Am. Chem. Soc.* **2012**, *134*, 12450–12453.

(4) (a) Du, J.; Chen, Y.; Zhang, Y.; Han, C.; Fischer, K.; Schmidt, M. Organic/Inorganic Hybrid Vesicles Based on a Reactive Block Copolymer. *J. Am. Chem. Soc.* **2003**, *125*, 14710–14711. (b) Du, J.; Tang, Y.; Lewis, A. L.; Armes, S. P. pH-Sensitive Vesicles Based on a Biocompatible Zwitterionic Diblock Copolymer. *J. Am. Chem. Soc.* **2005**, *127*, 17982–17983.

(5) Bangham, A. D. Liposomes: The Babraham Connection. *Chem. Phys. Lipids* **1993**, *64*, 275–285.

(6) Meng, F.; Zhong, Z.; Feijen, J. Stimuli-Responsive Polymersomes for Programmed Drug Delivery. *Biomacromolecules* **2009**, *10*, 197–209.

(7) Bellomo, E.; Wyrsta, G. M. D.; Pakstis, L.; Pochan, D. J.; Deming, T. J. Stimuli-responsive Polypeptide Vesicles by Conformation-Specific Assembly. *Nat. Mater.* **2004**, *3*, 244–248.

(8) Ahmed, F.; Pakunlu, R. I.; Brannan, A.; Bates, F.; Minko, T.; Discher, D. E. Biodegradable Polymersomes Loaded with Both Paclitaxel and Doxorubicin Permeate and Shrink Tumors, Inducing Apoptosis in Proportion to Accumulated Drug. *J. Controlled Release* **2006**, *116*, 150–158.

(9) Li, S.; Byrne, B.; Welsh, J.; Palmer, A. F. Self-Assembled Poly(butadiene)-*b*-Poly(ethylene oxide) Polymersomes as Paclitaxel Carriers. *Biotechnol. Prog.* **2007**, *23*, 278−285.
(10) Lomas, H.; Canton, I.; MacNeil, S.; Du, J.; Armes, S. P.; Ryan, A. J.; Lewis, A. L.; Battaglia, G. Biomimetic pH Sensitive Polymersomes for Efficient DNA Encapsulation and Delivery. *Adv. Mater.* **2007**, *19*, 4238−4243.
(11) Iatrou, H.; Frielinghaus, H.; Hanski, S.; Ferderigos, N.; Ruokolainen, J.; Ikkala, O.; Richter, D.; Mays, J.; Hadjichristidis, N. Architecturally Induced Multiresponsive Vesicles from Well-Defined Polypeptides. Formation of Gene Vehicles. *Biomacromolecules* **2007**, *8*, 2173−2181.
(12) Litvinchuk, S.; Lu, Z.; Rigler, P.; Hirt, T .D.; Meier, W. Calcein Release from Polymeric Vesicles in Blood Plasma and PVA Hydrogel. *Pharm. Res.* **2009**, *26*, 1711−1717.
(13) Onaca, O.; Enea, R.; Hughes, D. W.; Meier, W. Stimuli-Responsive Polymersomes as Nanocarriers for Drug and Gene Delivery. *Macromol. Biosci.* **2009**, *9*, 129−139.
(14) Ahmed, F. R.; Pakunlu, I.; Srinivas, G.; Brannan, A.; Bates, F.; Klein, M. L.; Minko, T.; Discher, D. E. Shrinkage of a Rapidly Growing Tumor by Drug-Loaded Polymersomes: pH-Triggered Release through Copolymer Degradation. *Mol. Pharmaceutics* **2006**, *3*, 340−350.
(15) Nishiyama, N.; Okazaki, S.; Cabral, H.; Miyamoto, M.; Kato, Y.; Sugiyama, Y. Novel Cisplatin-Incorporated Polymeric Micelles Can Eradicate Solid Tumors in Mice. *Cancer Res.* **2003**, *63*, 8977−8983.
(16) Stolnik, S.; Illum, L.; Davis, S. S. Long Circulating Micro particulate Drug Carriers. *Adv. Drug Delivery Rev.* **1995**, *16*, 195−214.
(17) Soo, P. L.; Eisenberg, A. Preparation of Block Copolymer Vesicles in Solution. *J. Polym. Sci., Part B: Polym. Phys.* **2004**, *42*, 923−938.
(18) Tokarczyk, K. K.; Grumelard, J.; Haefele, T.; Meier, W. Block Copolymer Vesicles Using Concepts from Polymer Chemistry to Mimic Biomembranes. *Polymer* **2005**, *46*, 3540−3563.
(19) Koide, A.; Kishimura, A.; Osada, K.; Jang, W. D.; Yamasaki, Y.; Kataoka, K. Semipermeable Polymer Vesicle (PICsome) Self-Assembled in Aqueous Medium from a Pair of Oppositely Charged Block Copolymers: Physiologically Stable Micro-/Nanocontainers of Water-Soluble Macromolecules. *J. Am. Chem. Soc.* **2006**, *128*, 5988−5989.
(20) Kishimura, A.; Koide, A.; Osada, K.; Yamasaki, Y.; Kataoka, K. Encapsulation of Myoglobin in PEGylated Polyion Complex Vesicle Made from a Pair of Oppositely Charged Block Ionomers: A Physiologically Available Oxygen Carrier. *Angew. Chem., Int. Ed.* **2007**, *46*, 6085−6088.
(21) Kabanov, A. V.; Bronich, T. K.; Kabanov, V. A.; Yu, K.; Eisenberg, A. Spontaneous Formation of Vesicles from Complexes of Block Ionomers and Surfactants. *J. Am. Chem. Soc.* **1998**, *120*, 9941−9942.
(22) Bronich, T. K.; Ouyang, M.; Kabanov, V. A.; Eisenberg, A.; Szoka, F. C.; Kabanov, A. V. Synthesis of Vesicles on Polymer Template. *J. Am. Chem. Soc.* **2002**, *124*, 11872−11873.
(23) Freese, C.; Gibson, M. I.; Klok, H.-A.; Unger, R. E.; Kirkpatrick, C. J. Size- and Coating-Dependent Uptake of Polymer-Coated Gold Nanoparticles in Primary Human Dermal Microvascular Endothelial Cells. *Biomacromolecules* **2012**, *13*, 1533−1543.
(24) Boyer, C.; Whittaker, M. R.; Nouvel, C.; Davis, T. P. Synthesis of Hollow Polymer Nanocapsules Exploiting Gold Nanoparticles as Sacrificial Templates. *Macromolecules* **2010**, *43*, 1792−1799.
(25) Banerjee. R.; Gupta, S.; Dey. D.; Maiti, S.; Dhara. D. Synthesis of PEG Containing Cationic Block Copolymers and Their Interaction with Human Serum Albumin. Manuscript submitted.
(26) Nisha, C. K.; Basak, P.; Manorama, S. V.; Maiti, S.; Jayachandran, K. N. Water-Soluble Complexes from Random Copolymer and Oppositely Charged Surfactant. 1. Complexes of Poly(ethylene glycol)-Based Cationic Random Copolymer and Sodium Dodecyl Sulfate. *Langmuir* **2003**, *19*, 2947−2955.
(27) Nisha, C. K.; Manorama, S. V.; Kizhakkedathu, J. N.; Maiti, S. Water-Soluble Complexes from Random Copolymer and Oppositely Charged Surfactant. 2. Complexes of Poly(ethylene glycol)-Based Cationic Random Copolymer and Bile Salts. *Langmuir* **2004**, *20*, 8468−8475.
(28) Kizhakkedathu, J. N.; Nisha, C. K.; Manorama, S. V.; Maiti, S. Water-Soluble Nanoparticles from Random Copolymer and Oppositely Charged Surfactant. *Macromol. Biosci.* **2005**, *5*, 549−558.
(29) Banerjee, R.; Maiti, S.; Dhara, D. Water-soluble Nanoparticles from Poly(ethylene glycol)-Based Cationic Random Copolymers and Double-Tail Surfactant. *Colloids Surf., A* **2012**, *395*, 255−261.
(30) Antonietti, M.; Forster, S.; Zisenis, M.; Conrad, J. Solution Viscosity of Polyelectrolyte−Surfactant Complexes: Polyelectrolyte Behavior in Nonaqueous Solvents. *Macromolecules* **1995**, *28*, 2270−2275.
(31) Kalyanasundaram, K.; Thomas, J. K. Environmental Effects on Vibronic Band Intensities in Pyrene Monomer Fluorescence and Their Application in Studies of Micellar Systems. *J. Am. Chem. Soc.* **1977**, *99*, 2039−2044.
(32) Burger, C.; Zhou, S.; Chu, B. *In Handbook of Polyelectrolytes and Their Applications*; Tripathy, S. K., Kumar, J., Nalwa, H. S., Eds.; American Scientific Publishers: Stevenson Ranch, CA, 2002; Vol. *3*, p 125.
(33) Bronich, T. K.; Kabanov, A. V. Soluble Complexes from Poly(ethylene oxide)-*block*-Polymethacrylate Anions and *N*-Alkylpyridinium Cations. *Macromolecules* **1997**, *30*, 3519−3525.
(34) Israelachvili, J. In *Intermolecular & Surface Forces*, 2nd ed.; Academic Press: London, 1991.
(35) Yamamoto, H.; Mizusaki, M.; Yoda, K.; Morishima, Y. Fluorescence Studies of Hydrophobic Association of Random Copolymers of Sodium 2-(Acrylamido)-2-methylpropanesulfonate and *N*-Dodecylmethacrylamide in Water. *Macromolecules* **1998**, *31*, 3588−3594.
(36) Yamamoto, H.; Morishima, Y. Effect of Hydrophobe Content on Intra- and Interpolymer Self-Associations of Hydrophobically Modified Poly(sodium 2-(acrylamido)-2-methylpropanesulfonate) in Water. *Macromolecules* **1999**, *32*, 7469−7475.
(37) Solomatin, S. V.; Bronich, T. K.; Bargar, T. W.; Eisenberg, A.; Kabanov, V. A.; Kabanov, A. V. Environmentally Responsive Nanoparticles from Block Ionomer Complexes: Effects of pH and Ionic Strength. *Langmuir* **2003**, *19*, 8069−8076.
(38) Mantzaridis, C.; Mountrichas, G.; Pispas, S. Complexes between High Charge Density Cationic Polyelectrolytes and Anionic Single- and Double-Tail Surfactants. *J. Phys. Chem. B* **2009**, *113*, 7064−7070.
(39) Sakai, T.; Alexandridis, P. Single-Step Synthesis and Stabilization of Metal Nanoparticles in Aqueous Pluronic Block Copolymer Solutions at Ambient Temperature. *Langmuir* **2004**, *20*, 8426−8430.
(40) Sakai, T.; Alexandridis, P. Spontaneous Formation of Gold Nanoparticles in Poly(ethylene oxide)−Poly(propylene oxide) Solutions: Solvent Quality and Polymer Structure Effects. *Langmuir* **2005**, *21*, 8019−8025.
(41) Sakai, T.; Alexandridis, P. Mechanism of Gold Metal Ion Reduction, Nanoparticle Growth and Size Control in Aqueous Amphiphilic Block Copolymer Solutions at Ambient Conditions. *J. Phys. Chem. B* **2005**, *109*, 7766−7777.
(42) Chen, S.; Guo, C.; Hu, G. H.; Wang, J.; Ma, J. H.; Liang, X. F.; Zheng, L.; Liu, H. Z. Effect of Hydrophobicity inside PEO−PPO−PEO Block Copolymer Micelles on the Stabilization of Gold Nanoparticles: Experiments. *Langmuir* **2006**, *22*, 9704−9711.
(43) Sabir, T. S.; Yan, D.; Milligan, J. R.; Aruni, A. W.; Nick, K. E.; Ramon, R. H.; Hughes, J. A.; Chen, Q. R.; Kurti, S.; Perry, C. Kinetics of Gold Nanoparticle Formation Facilitated by Triblock Copolymers. *J. Phys. Chem. C* **2012**, *116*, 4431−4441.
(44) Rahme, K.; Gauffre, F.; Marty, J.-D.; Payre, B.; Mingotaud, C. A Systematic Study of the Stabilization in Water of Gold Nanoparticles by Poly(Ethylene Oxide)-Poly(Propylene Oxide)-Poly(Ethylene Oxide) Triblock Copolymers. *J. Phys. Chem. C* **2007**, *111*, 7273−7279.
(45) Goy-López, S.; Taboada, P.; Cambón, A.; Juárez, J.; Alvarez-Lorenzo, C.; Concheiro, A.; Mosquera, V. Modulation of Size and Shape of Au Nanoparticles Using Amino-X-Shaped. Poly(ethylene

oxide)-Poly(propylene oxide) Block Copolymers. *J. Phys. Chem. B* **2010**, *114*, 66−76.
(46) Polte, J.; Emmerling, F.; Radtke, M.; Reinholz, U.; Riesemeier, H.; Theunemann, A. F. Real-Time Monitoring of Copolymer Stabilized Growing Gold Nanoparticles. *Langmuir* **2010**, *26*, 5889−5894.
(47) Khullar, P.; Mahal, A.; Singh, V.; Banipal, T. S.; Kaur, G.; Bakshi, M. S. How PEO-PPO-PEO Triblock Polymer Micelles Control the Synthesis of Gold Nanoparticles: Temperature and Hydrophobic Effects. *Langmuir* **2010**, *26*, 11363−11371.
(48) Yuan, Y.-Y.; Liu, X.-Q.; Wang, Y.-C.; Wang, J. Gold Nanoparticles Stabilized by Thermosensitive Diblock Copolymers of Poly(ethylene glycol) and Polyphosphoester. *Langmuir* **2009**, *25*, 10298−10304.
(49) Goy-López, S.; Castro, E.; Taboada, P.; Mosquera, V. Block Copolymer-Mediated Synthesis of Size-Tunable Gold Nanospheres and Nanoplates. *Langmuir* **2008**, *24*, 13186−13196.
(50) Haba, Y.; Kojima, C.; Harada, A.; Ura, T.; Horinaka, H.; Kono, K. Preparation of Poly(ethylene glycol)-Modified Poly(amido amine) Dendrimers Encapsulating Gold Nanoparticles and Their Heat-Generating Ability. *Langmuir* **2007**, *23*, 5243−5246.